

Detecting fractures using time-lapse 3C-3D seismic data

Zimin Zhang, Don C. Lawton and Robert R. Stewart

ABSTRACT

This report presents the interpretation of time-lapse 3C-3D seismic data for fracture detection in a Saskatchewan potash mine. Seismic interpretation of the time-lapse 3C-3D surveys saw noticeable amplitude changes and time delay effects at the Dawson Bay and underlying formations in the 2008 survey compared with the 2004 survey, especially on the converted-wave (P-to-S) data. V_p/V_s analysis displayed increasing values on the 2008 survey within a faulted part of the survey area. Seismic curvature attributes were calculated at the top of the Dawson Bay Formation and the mining level. The curvatures also suggest that the fractures are well developed in parts of the Dawson Bay Formation.

INTRODUCTION

Geology background and previous study

A major problem for potash mining can be brine inflow. This may cause ore loss and operational problems. In the Saskatchewan mining area studied, potash ore (used in fertilizer and other products) is situated 20-30m from the top of a 100-200m thick salt unit (Zhang and Stewart, 2009) in the Prairie Evaporite Formation which is present through much of the Williston Basin region (Fuzesy, 1982). Above the mining interval, there can be aquifers at the bottom of the Souris River Formation and upper part of the Dawson Bay (Figure 1). Between the aquifers and ore zone, the formation is composed of shale, dolomite and dolomitized limestone. These rocks may be fractured and any fracturing of normally impermeable carbonate rocks could create a brine inflow path that might compromise potash mining operations.

An effective way to mitigate the risk posed by brine flows is to map and predict the volume and location of potentially affected areas prior to mining. To investigate the feasibility of using multi-component and repeated (time-lapse) seismic methods for crack mapping and monitoring, rock-physics modeling and synthetic seismogram were used to predict seismic velocity changes and seismic signatures of cracks in the Dawson Bay formation (Zhang and Stewart, 2009). The results indicate that P-wave and S-wave velocities will decrease (often significantly) with cracks or fractures. Vertically aligned cracks may also display azimuthal anisotropy. Synthetic seismograms calculated using the original well logs and those with cracks show observable changes such as “push-down” effects or time lags and amplitude variations with offset. By anisotropic numerical seismic modeling method (Zhang et al., 2010), using a fractured model based on well logs associated with potash mining, found that azimuthal seismic anisotropy and shear-wave splitting were effective in detecting/delineating the fractures.

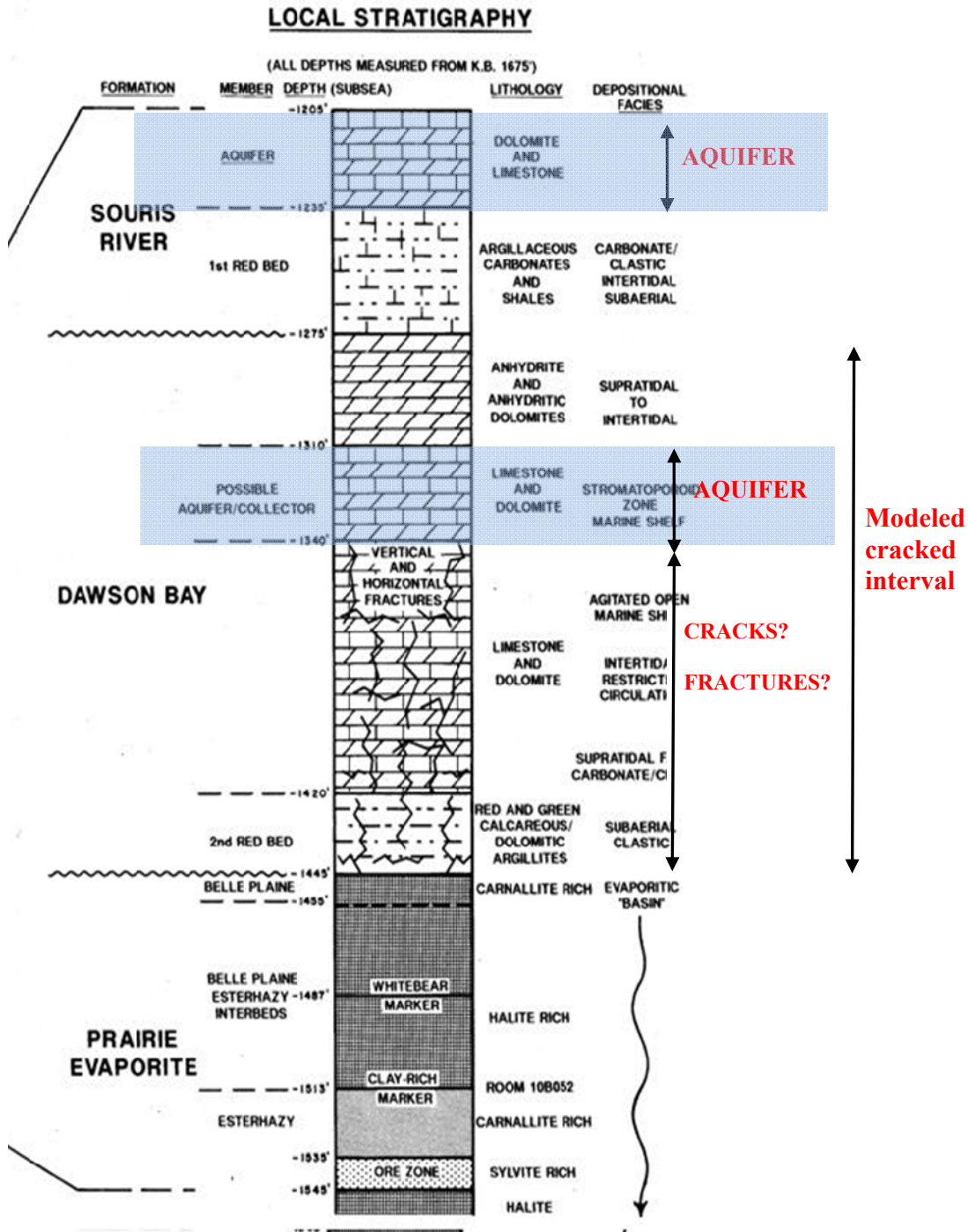


FIG 1. Local stratigraphy of Prairie Evaporite and overlying formations in the mining area. The Dawson Bay carbonates, dolomites, and shales can host fractures (from R. Edgcombe, personal communication, 2008).

Time-lapse 3C-3D seismic data

To assess the brine inflow problem, seven 3D seismic surveys, including five 3C surveys, were shot from 2003 to 2008 in the mining area. In 2009, two 3C-3D surveys, which were acquired in 2004 and 2008, were processed to monitor and

characterize the brine inflow. FIG 2 shows the location of the processed time-lapse (2004 and 2008) 3C-3D surveys in the mining area. A particular area, known as the “trap door” outlined in red is the main interpreted area of brine inflow. The size of the survey is about 6.5 km². The processing workflow is shown in FIG 3 (Sensor Geophysical of Calgary). In this report, the field time-lapse 3C-3D seismic data was interpreted to delineate fractured zones.

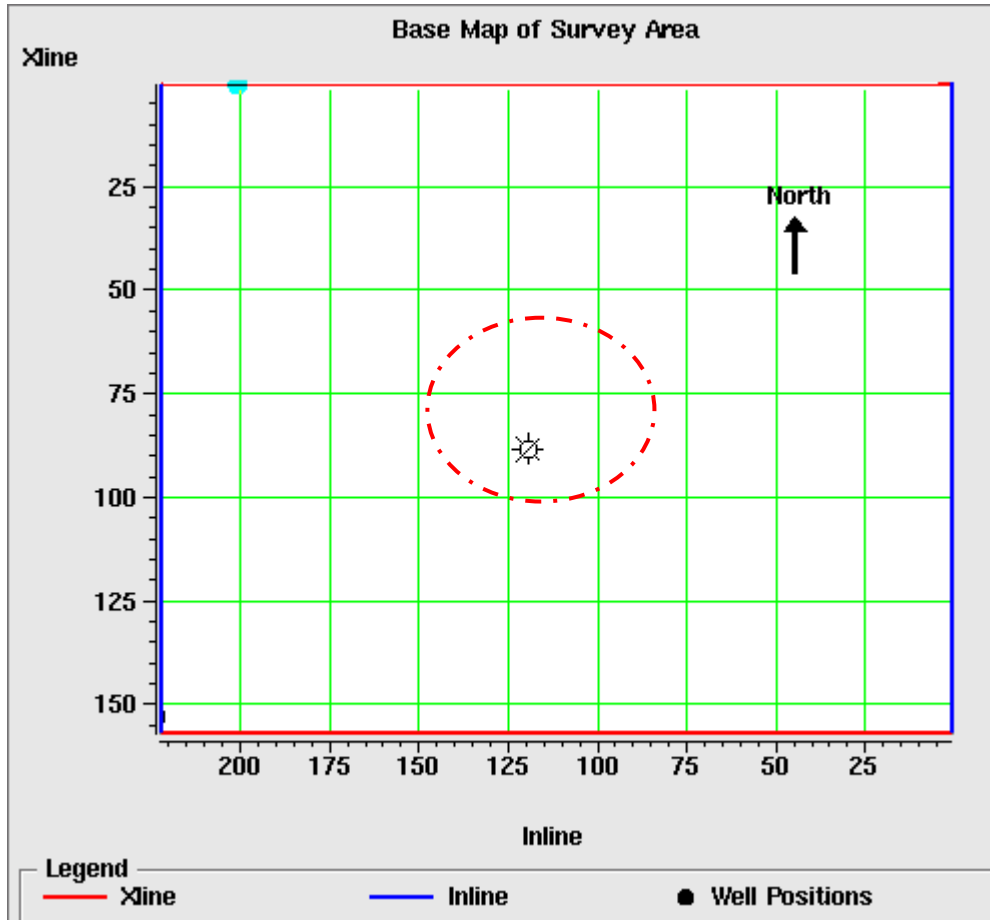


FIG 2. The time-lapse 3C-3D survey map. The red circle outlines the “trap door” area (where time delays of interpreted from seismic reflections around the mining level were caused possibly by brine inflow) interpreted from previous work (from John Boyd, personal communication, 2010).

```
C05 Record Length: 3.0 s Sample Interval: 1 ms
C06 Source: Dyn, single hole, 0.5 Kg at 9 m, N-S 125 m lines, 30 m source int
C07 Sensors: ION SM-7, single 3-comp, 0 degrees, E-W 180 m lines, 25 m int
C08 Typical Patch: 14 lines x 110 stations, 2340 m x 2725 m
C09 RADIAL LAYER STRIPPED FILTERED MIGRATED STACK
C10 *** Processing History ***
C11 Processed by: Sensor Geophysical Ltd., July, 2009
C12 Reformat: Record length 3.0 s, Sample interval 1.0 ms
C13 Geometry Assignment, Asymptotic 3D Binning, CDP Bin size 12.5 m x 15 m
C14 H1/H2 to Radial/Transverse Rotation: 7 degrees, Trace edits, 60 Hz removal
C15 Amplitude Recovery: Spherical divergence correction, Additional gain 4 dB/s
C16 Surface-Consistent Deconvolution
C17 Resolved: Source, Receiver, Offset Applied: Source, Receiver
C18 Operator Type Spiking, Operator length 100 ms, Prewhitening 0.01%
C19 Design window 120-2300 ms at 0 m, 1000-2500 ms at 2170 m offset
C20 Time-Variant Spectral Whitening: 2/6-80/100 Hz, 7 panels, 500 ms operator
C21 Lateral Receiver Statics, Refraction Statics: Datum elev 620m, Repl vel 2000
C22 Surface Consistent Statics: Max shift 24 ms, 400-2200 ms, CDP Trim Statics
C23 Anisotropic Normal Moveout Correction: eta 0.1
C24 Front-End Muting: Mute time (ms) 0 400 2300 Offset (m) 300 375 2125
C25 Limited Azimuth Stacks: 10-360(10) degrees, AGC
C26 PS1/PS2 Analysis: 500-900, 900-1250, 1500-1900 ms
C27 RAD/TRS to RAD 3 Layers Stripped Rotation
C28 3D CCP Stack: Effective vp/vs = 60% Vertical vp/vs, bulk shift 0 ms
C29 Time-Variant Spectral Whitening: 2/6-60/80 Hz, 6 panels, 500 ms operator
C30 Trace Equalization: Mean window 400-3000 ms
C31 F-XY Filtering, 5x5 point operator, 100 ms window, 50 ms taper
C32 Diffusion Filter
C33 Migration: Implicit FD Time, Aperture 65 degrees, 95% smoothed stacking vels
C34 Bandpass Filter, Zero-phase Ormsby, 5/10-30/40 Hz
C35 Time Variant Scaling: mean, centre-to-centre, multiple gates
C36
```

CDP Bin size: 12.5m X 15m

FIG 3. Processing workflow used for the time-lapse 3C-3D seismic data (from Sensor Geophysical Ltd.).

INTERPRETATION OF TIME-LAPSE 3C-3D SURFACE SEISMIC DATA

Well-seismic correlation and PP - PS data registration

We first proceeded to correlate the wells to the 3C-3D seismic data before interpreting the seismic data. FIG 4 displays the correlation between the synthetic PP seismogram of well GROUT 59-1 and the migrated PP data of the 2004 survey. The P-wave synthetic seismogram ties fairly well with the PP field seismic section. Then, the PS synthetic seismogram was tied to the field PS seismic data (FIG 5). Again, a reasonable correlation was found. The PP and PS sections (FIG 6 and FIG 7) were then registered for both 2004 and 2008 surveys. The difference between the frequency bandwidth of the PP data and the PS data is significant. The effective frequency of the P-wave data is up to 120Hz, while it is only about 60Hz with the PS events. The reflections of the interfaces of porous zone, the Dawson Bay Formation, and the Prairie Evaporite Formation within the target zone can all be recognized (FIG 4, FIG 5, and FIG 8). However, due to the frequency difference, they are not easily picked on the radial data individually. Therefore, to pick the PP and PS horizons at exactly the same depth is particularly difficult. However, the structure from PP and PS data can still represent relative features despite of the picking errors.

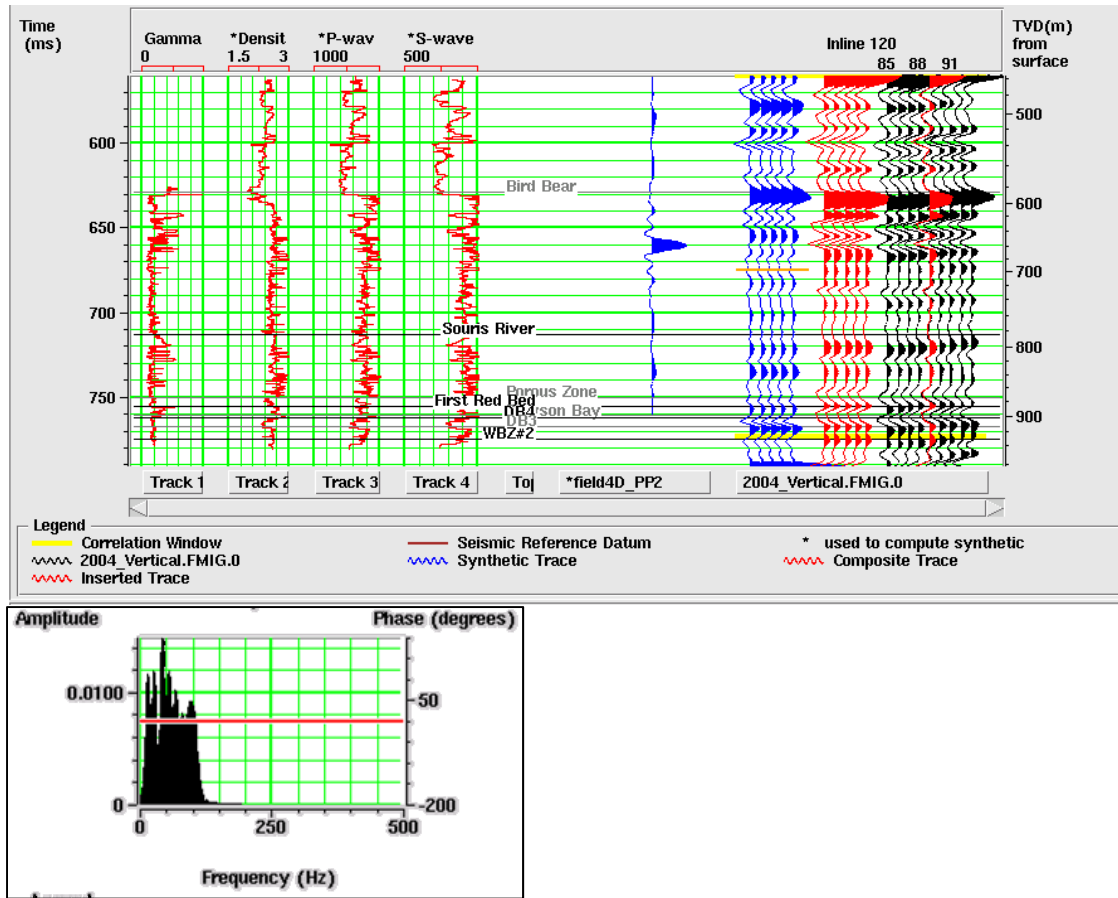


FIG 4. Correlation between the synthetic PP seismogram of well GROUT 59-1 and migrated PP data of 2004 survey. The synthetic seismogram is displayed in blue and repeated for 5 times, the seismic traces adjacent to the well are displayed in black. The corresponding frequency spectrum is shown at the bottom.

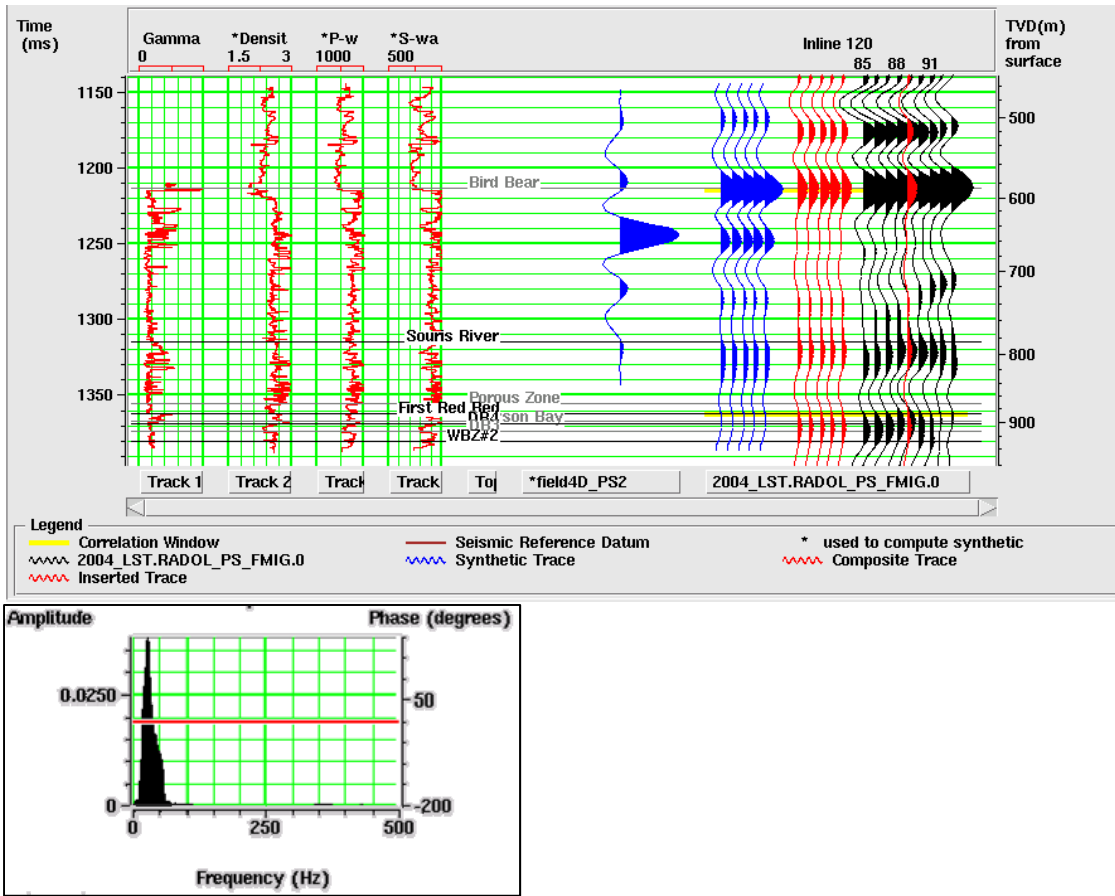


FIG 5. Correlation between the synthetic PS seismogram of well GROUT 59-1 and migrated PS data of 2004 survey. The synthetic seismogram is displayed in blue and repeated for 5 times, the seismic traces adjacent to the well are displayed in black. The corresponding frequency spectrum is shown at the bottom.

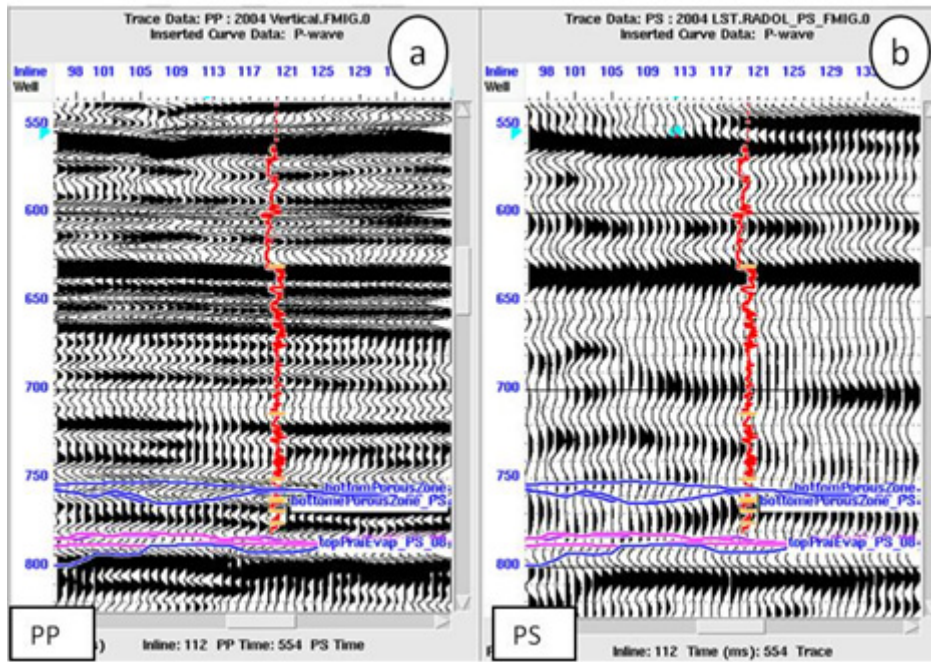


FIG 6. Registration of the PP data and PS data of the 2004 survey, both data are in PP time. The picked horizon at about 750ms is the base of the porous zone, and the horizon at about 800ms is approximated the top of Prairie Evaporite Formation. The horizontal bars on the well log curve are the geological markers.

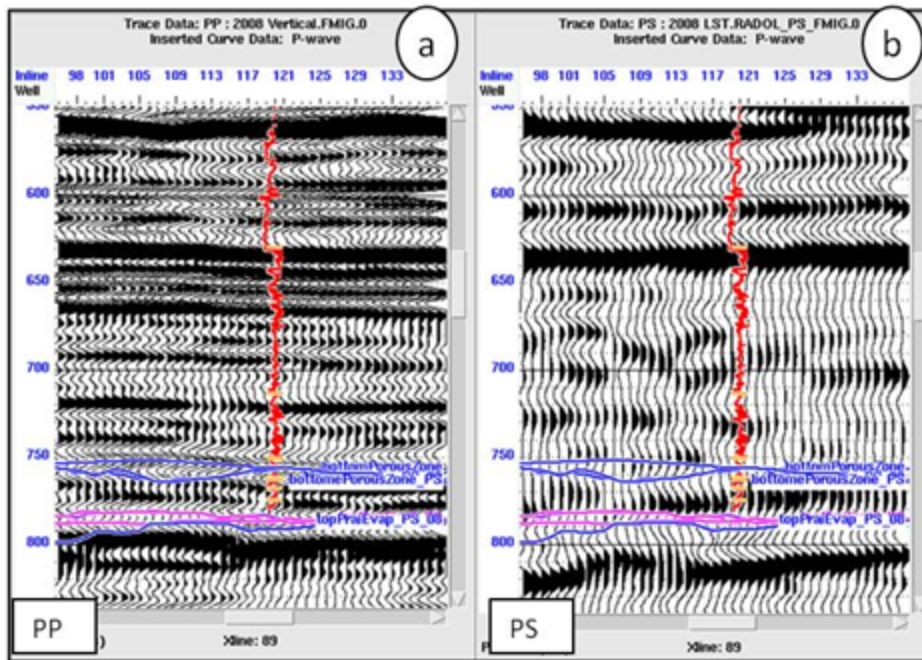


FIG 7. Registration of PP data (a) and PS data (b) of the 2008 survey, both data are in PP time. The picked horizon at about 750ms is the base of the porous zone, and the horizon at about 800ms is approximately the top of Prairie Evaporite Formation. The horizontal bars on the well log curve are the geological markers.

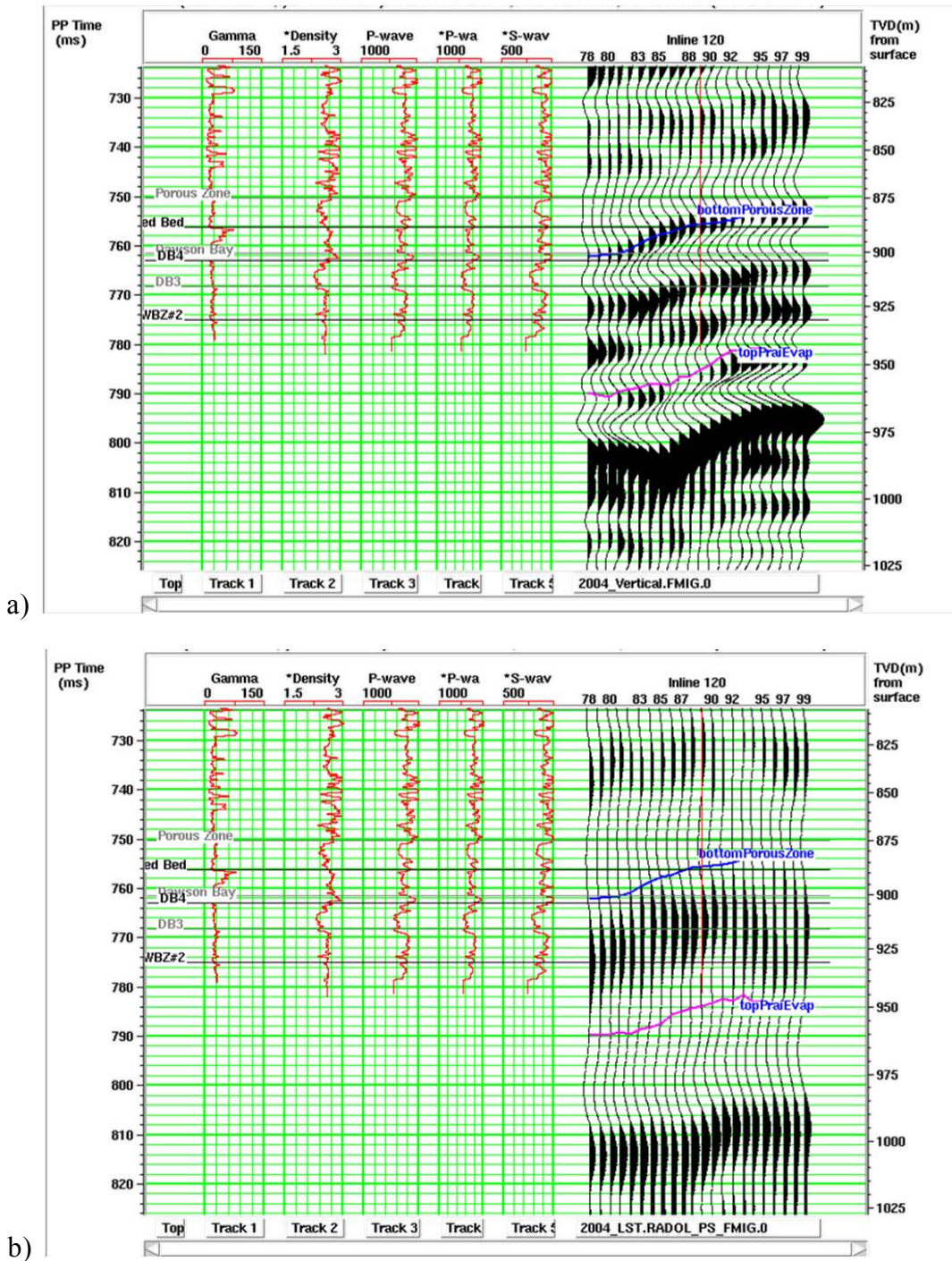


FIG 8. The base of the Porous Zone and the base of the Dawson Bay Formation picks and the correlation with well logs. On the vertical component, the base of the Porous Zone is a peak, the base of the Dawson Bay Formation corresponds to a zero-crossing point on seismic traces. On the radial component, there are no accurate picks for the two geological markers due to low resolution. Approximately they correspond to two zero-crossing points.

Time-lapse interpretation

FIG 9 and FIG 10 display the PP data and the PS data from an west-east line from the two 3D surveys. There are visible changes such as time shift and amplitude difference on both PP and PS data, especially within the red ellipse in the figures. Both components show apparent push-down effects due to a velocity decrease between the 2004 and 2008 surveys. Amplitude dimming can be seen at the Dawson Bay Formation in the 2008 PS data compared with the 2004 survey. Difference data between the 2004 and 2008 survey were also calculated after applying a match filter derived in the 420-620 ms widow for PP data, and 600-1250 ms for PS data. The difference is relatively small for PP data. Based on the rock physics modeling result, the reason should be a small P-wave velocity change when fractures exist in the formation. However, in the trap door area some differences can still be found. On the PS data, an apparent difference can be seen below the Dawson Bay Formation (the bottom is approximately the green horizon on the seismic line). All these features are consistent with the modeling results: when fractures exist in the formation, a significantly greater decrease of S-wave velocity than the P-wave velocity will be observed. FIG 11 also displays the RMS amplitude difference between the two surveys for the Dawson Bay Formation. There were two main areas where fractures might exist in the Dawson Bay Formation, one is outlined by blue circles and the other is shown in red circles. The area of change (red circle) is also observed on the PP and PS data in FIG 9 and FIG 10, respectively. An evident push-down effect can be seen in this region.

To investigate the time shift caused by the changes in the Dawson Bay Formation, the top and the bottom of the Dawson Bay Formation were picked to see the time structure changes between the 2004 and 2008 surveys. Due to the low frequency of the PS data, however, the base of the Dawson Bay Formation, which is also the top of the Prairie Evaporite Formation, was difficult to pick. Therefore, on the PS data, the mine level was picked. FIG 12 and FIG 13 show the time structure on the top of the Dawson Bay Formation. The difference on PP data is fairly small. A visible difference can also be seen on the PS data, pull-up effect appears at the top of the Dawson Bay Formation in the 2008 survey compared with the 2004 survey. Since the difference between the two surveys of the Birdbear Formation is fairly small (FIG 14 and FIG 15), it indicates that some changes occurred between the Birdbear Formation and the Dawson Bay Formation.

At the base of the Dawson Bay Formation, the time structure of the PP data shows mostly of push-down on the 2008 data (Figure 16). However, the time-shift is only up to about 2ms. On the PS data, a significant time-shift (push-down) can be seen at the mining level (Figure 17). The time shift can exceed 10ms. The modeling of fractures in the Dawson Bay Formation indicates that the P velocity will decrease less than the S-velocity, so the time-shift of PS data caused by fractures should be much larger than that of the PP data. Considering the time-shift values of the PP and PS data, it is interpreted that the rocks between the top of Prairie Evaporite Formation and mine level may also be fractured.

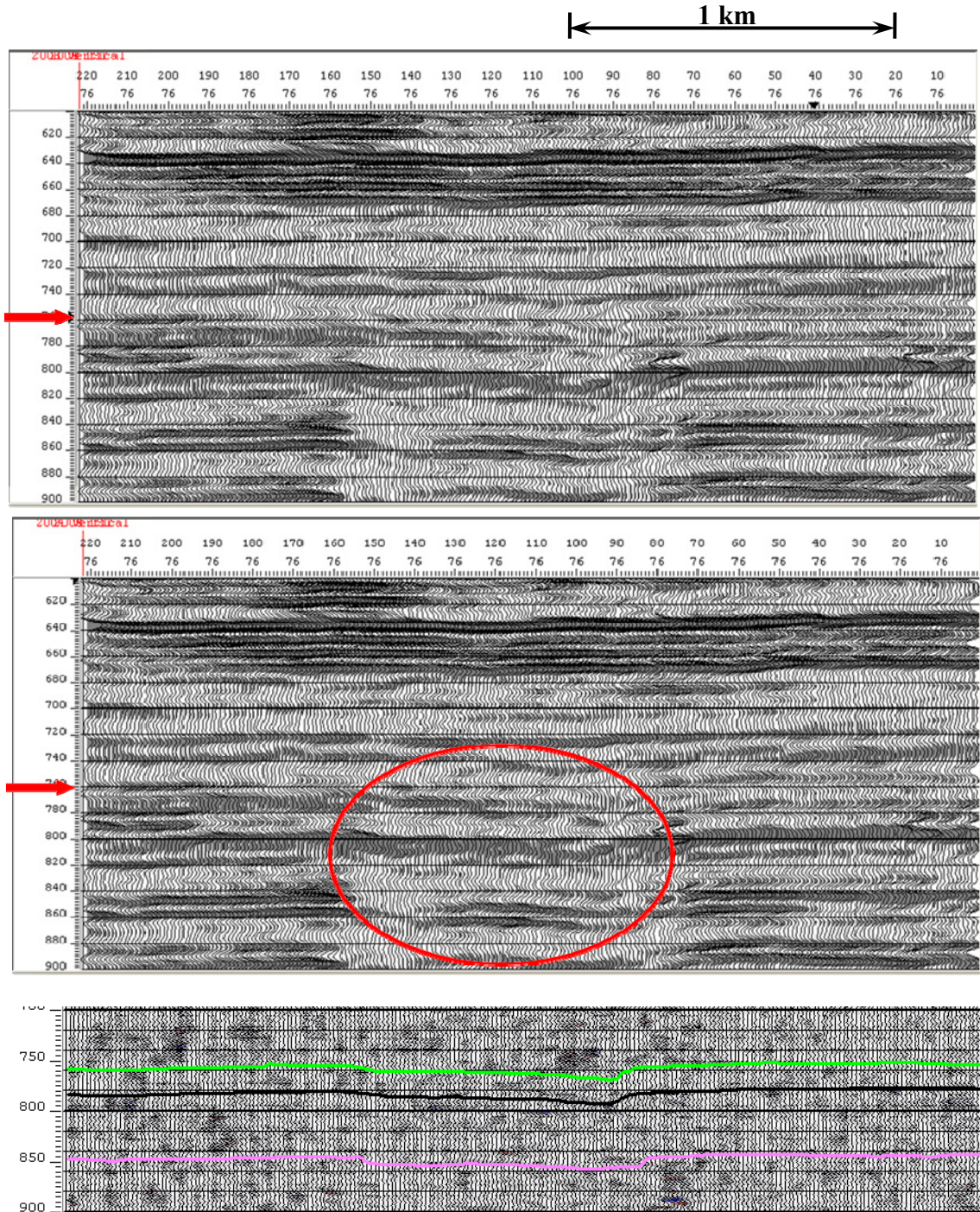


FIG 9. PP data of a west-east line. Top: 2004 survey; middle: 2008 survey; bottom: difference between the two data sets. The red arrows mark the location of the top of the Dawson Bay Formation. The red ellipse denotes the trap door area.

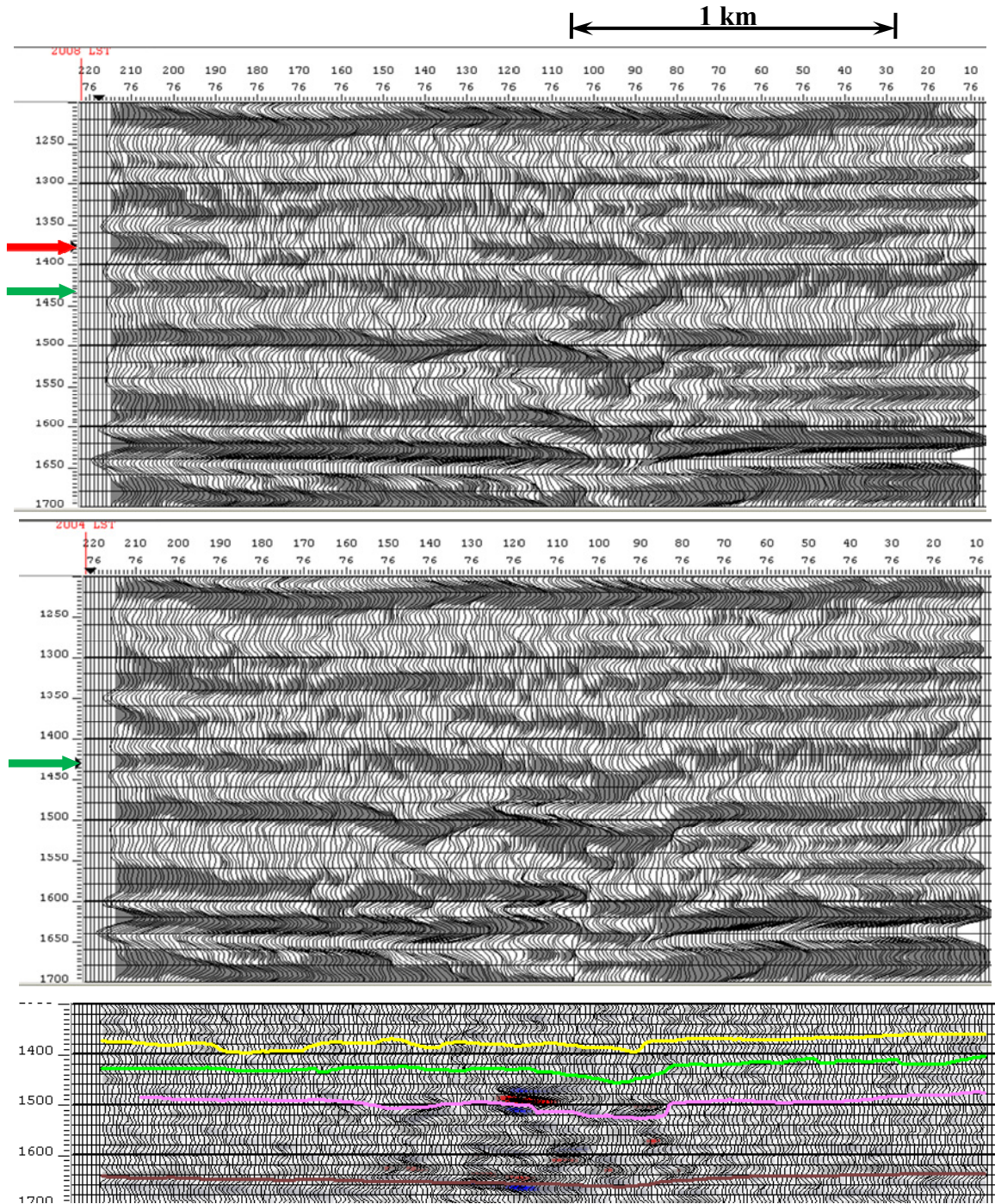


FIG 10. PS data of a west-east line. Top: 2004 survey; middle: 2008 survey; bottom: difference between the two data sets. The red arrows mark the location of the top of the Dawson Bay Formation. The green arrows are the mining zone. The trap door area is outlined by red ellipse.

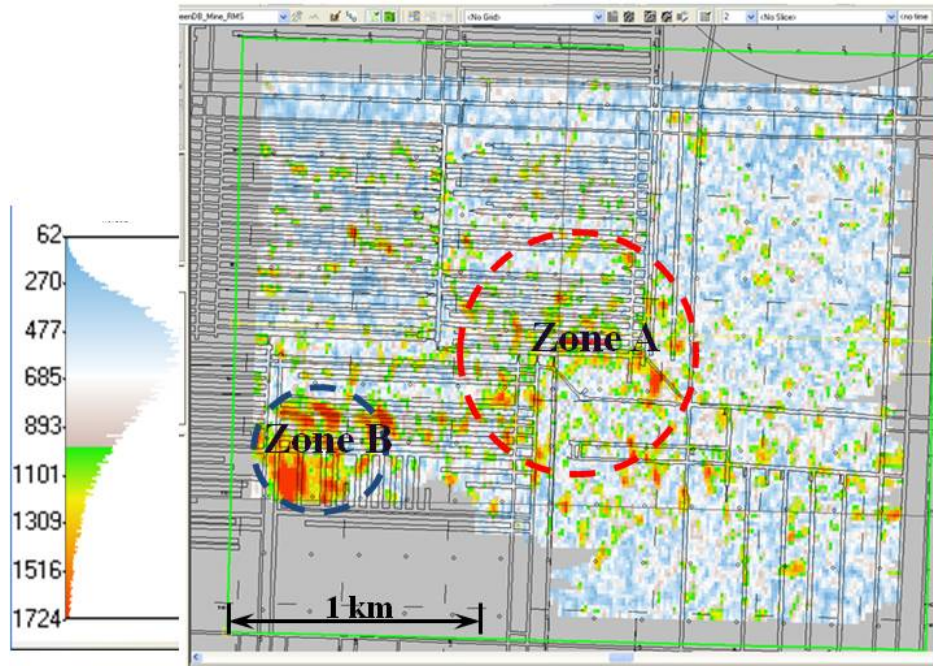


FIG 11. RMS amplitude difference of PS data from the Dawson Bay Formation to mine level between 2004 and 2008 survey.

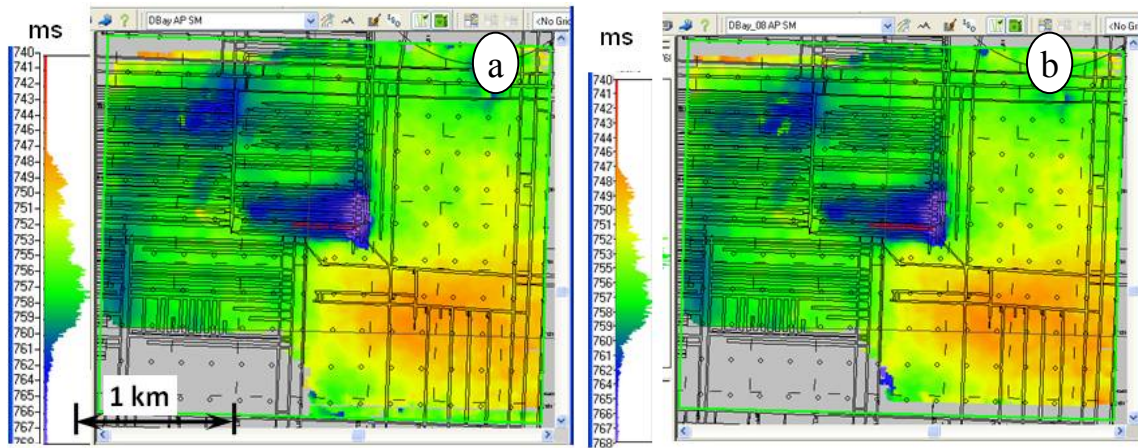


FIG 12. Time structure of the top of the Dawson Bay Formation on the PP data. a: 2004 survey; b: 2008 survey.

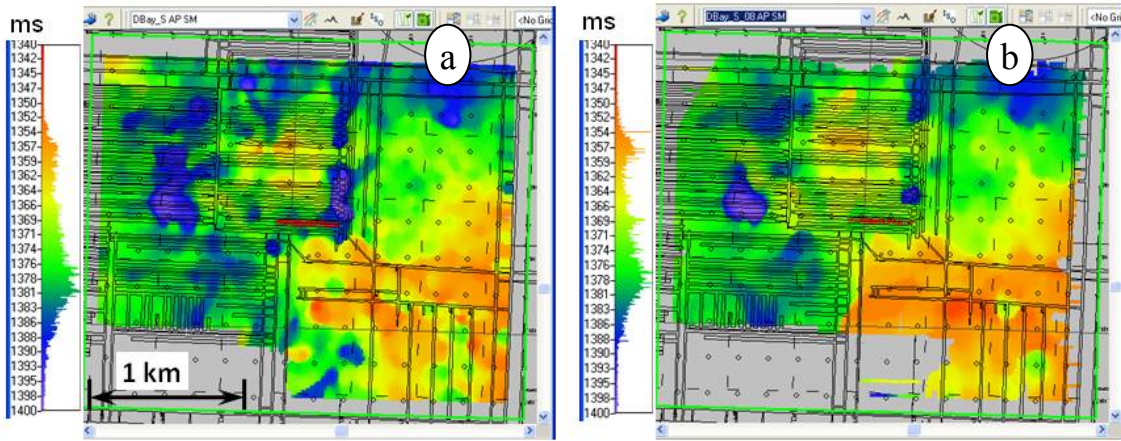


FIG 13. Time structure of the top of the Dawson Bay Formation on the PS data, a: 2004 survey; b: 2008 survey.

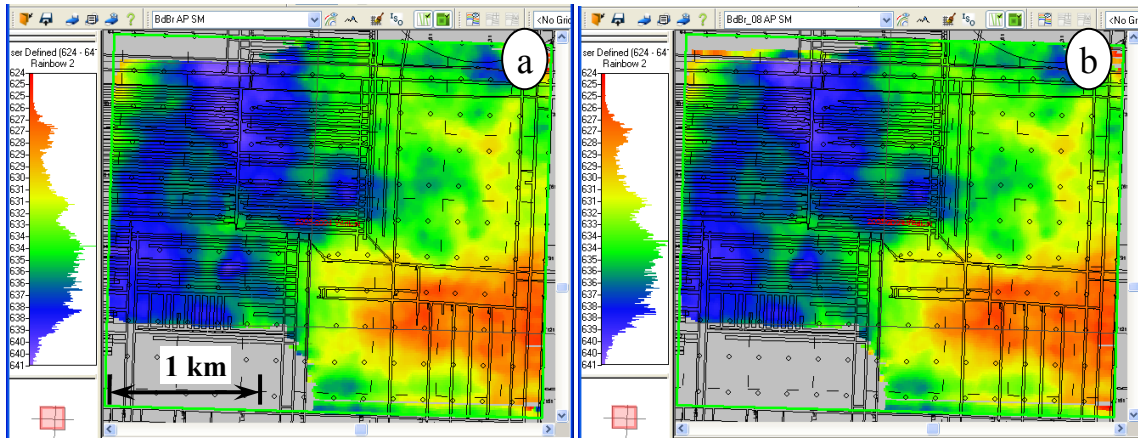


FIG 14. Time structure of the top of the Birdbear Formation on the PP data, a: 2004 survey; b: 2008 survey. There is almost no time shift between the two surveys.

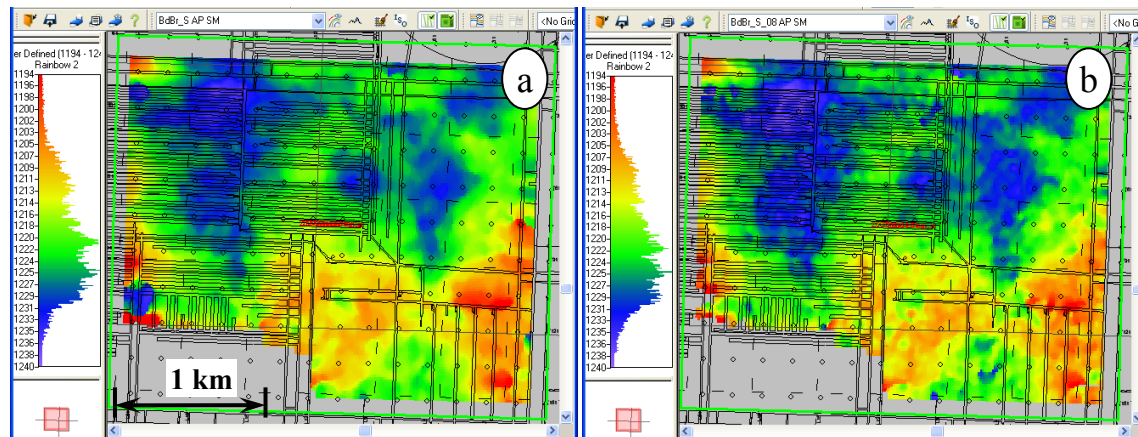


FIG 15. Time structure of the top of the Birdbear Formation on the PS data, a: 2004 survey; b: 2008 survey. The time shift between the two surveys is fairly small. A little delay was found on 2008 survey.

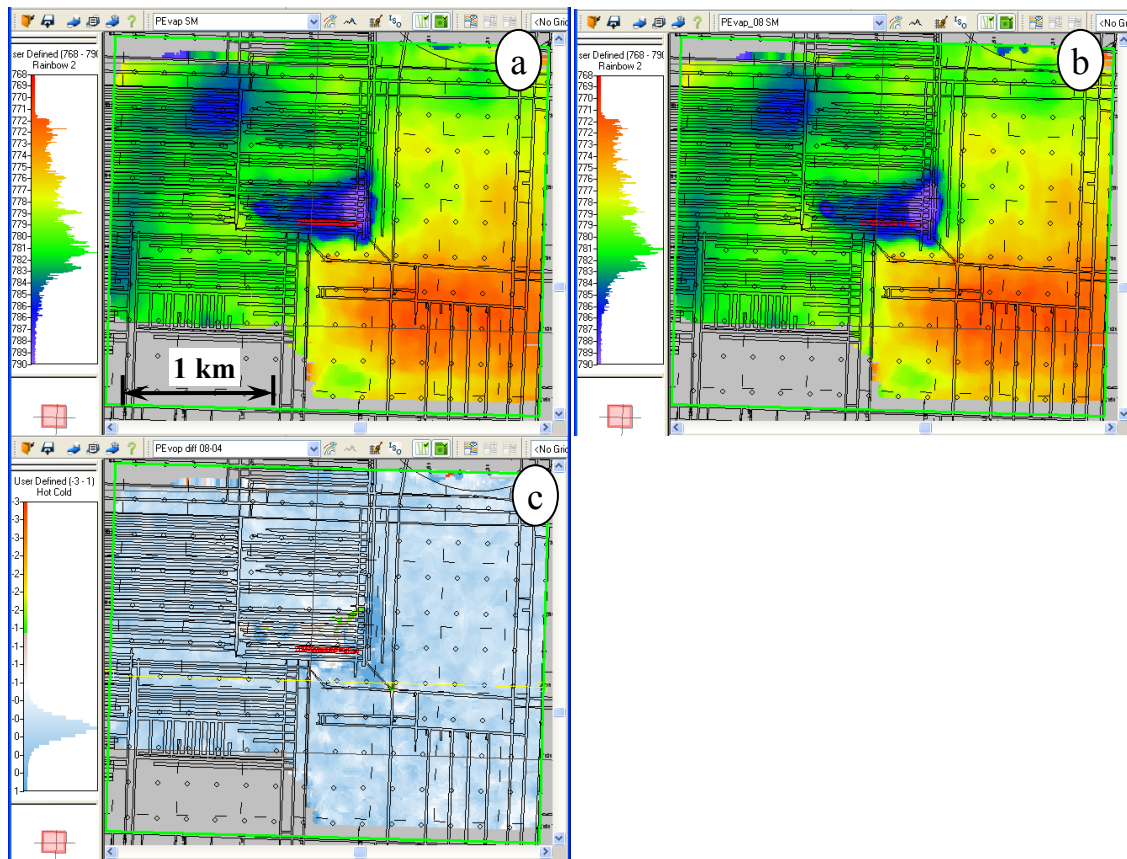


FIG 16. Time structure of the top of the Prairie Evaporite Formation on the PP data, a: 2004 survey; b: 2008 survey; c: PP travel time difference at the top of the Prairie Evaporite Formation between 2008 and 2004 survey.

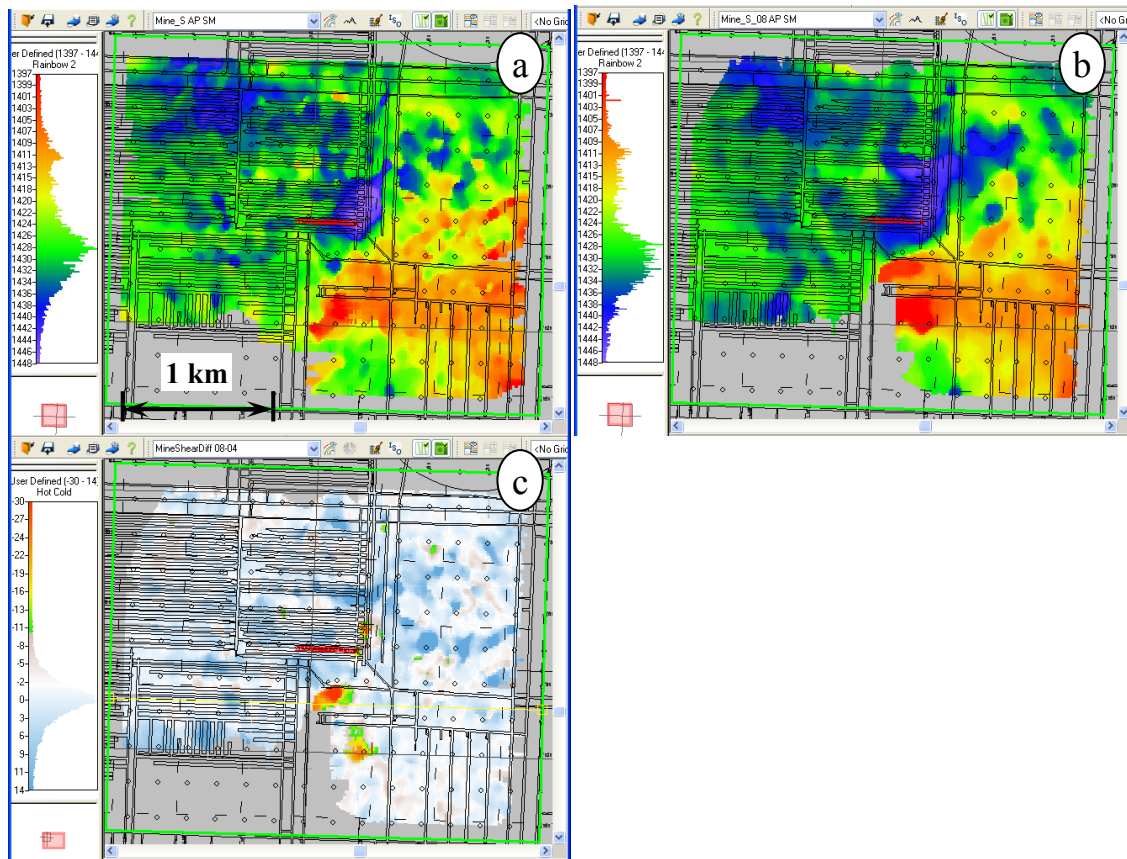


FIG 17. Time structure of the mine level on the PS data, a: 2004 survey; b: 2008 survey; c: PS travel time difference at the mine level between 2008 and 2004 survey.

According to our rock physics modeling, V_p/V_s will increase when fractures are present in the Dawson Bay Formation due to relatively larger decrease in the S-wave velocity compared with the P-wave velocity. Therefore, an interval V_p/V_s map of the Dawson Bay Formation may be used as an indicator of fractures in the formation. The V_p/V_s maps were constructed using the isochron maps from both PP and PS data for the same interval according to the formula (Margrave et al., 1998),

$$\frac{v_p}{v_s} = \frac{2\Delta t_{ps} - \Delta t_{pp}}{\Delta t_{pp}} \quad (1)$$

where Δt_{ps} , and Δt_{pp} are the PS and PP isochron maps for a particular interval.

Considering the difficulty in accurately picking the top and the base of the Dawson Bay Formation as well as robust V_p/V_s calculation, two intervals were chosen for interval V_p/V_s analysis using equation (1): interval 1 is from the Birdbear Formation to the Dawson Bay Formation, and interval 2 is from the Birdbear Formation to (approximately) the Shell Lake anhydrite below the Dawson Bay Formation (FIG 18). By comparing the V_p/V_s maps of these two intervals, the

relative changes in the Vp/Vs trend caused by the Dawson Bay Formation can be approximately estimated.

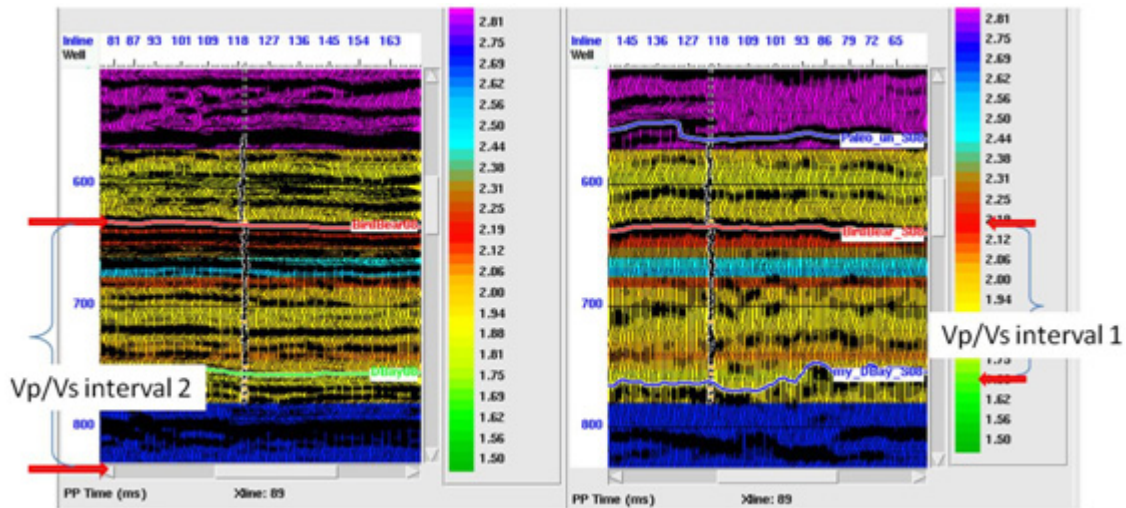


FIG 18. The arrow marks the intervals used for interval Vp/Vs calculation. Interval 1 is from the Birdbear Formation to the Dawson Bay Formation; interval 2 is from the Birdbear Formation to (approximately) the Shell Lake anhydrite below the Dawson Bay Formation (Vp/Vs extrapolated from well values superimposed on the seismic sections).

From FIG 19, it can be found that there is almost no variation of interval Vp/Vs values between the two surveys from the Birdbear Formation to the Dawson Bay Formation. About a 10% Vp/Vs increase is observed within the trap door area (outlined by red ellipse) on the interval Vp/Vs values of 2008 data from the Birdbear Formation to the Shell Lake anhydrite (FIG 20). These results indicate that: 1) above the Dawson Bay Formation, there are no fractures created between 2004 and 2008; 2) it is interpreted that fractures may have developed in the strata from the Dawson Bay Formation to the Shell Lake anhydrite between 2004 and 2008. A west-east line across the south edge of the trap door area was chosen for detailed interval Vp/Vs analysis of the Dawson Bay Formation (FIG 21). The Vp/Vs values of the Dawson Bay Formation for the 2004 survey are around 2.0. In the 2008 survey, a generally increasing trend of Vp/Vs can be seen, especially from CDP 80 to CDP 140, which is in the trap door area. The Vp/Vs increase suggests a larger S-wave velocity decrease caused by fractures in the formation. However, the Vp/Vs values seem to be too large (Vp/Vs for carbonate is 1.8). It could be attributed to the large picking errors of the top and the base of the Dawson Bay Formation on the PS data (which is also the top of Prairie Evaporite Formation) due to the low frequency content. Since the horizon picked on seismic data follows distinct wavelet features, such as a peak, trough, or zero crossing, it is unlikely that PP and PS picks will coincide consistently in depth. It will also cause deviation between the Vp/Vs values estimated from seismic data and real values (Margrave et al., 1998).

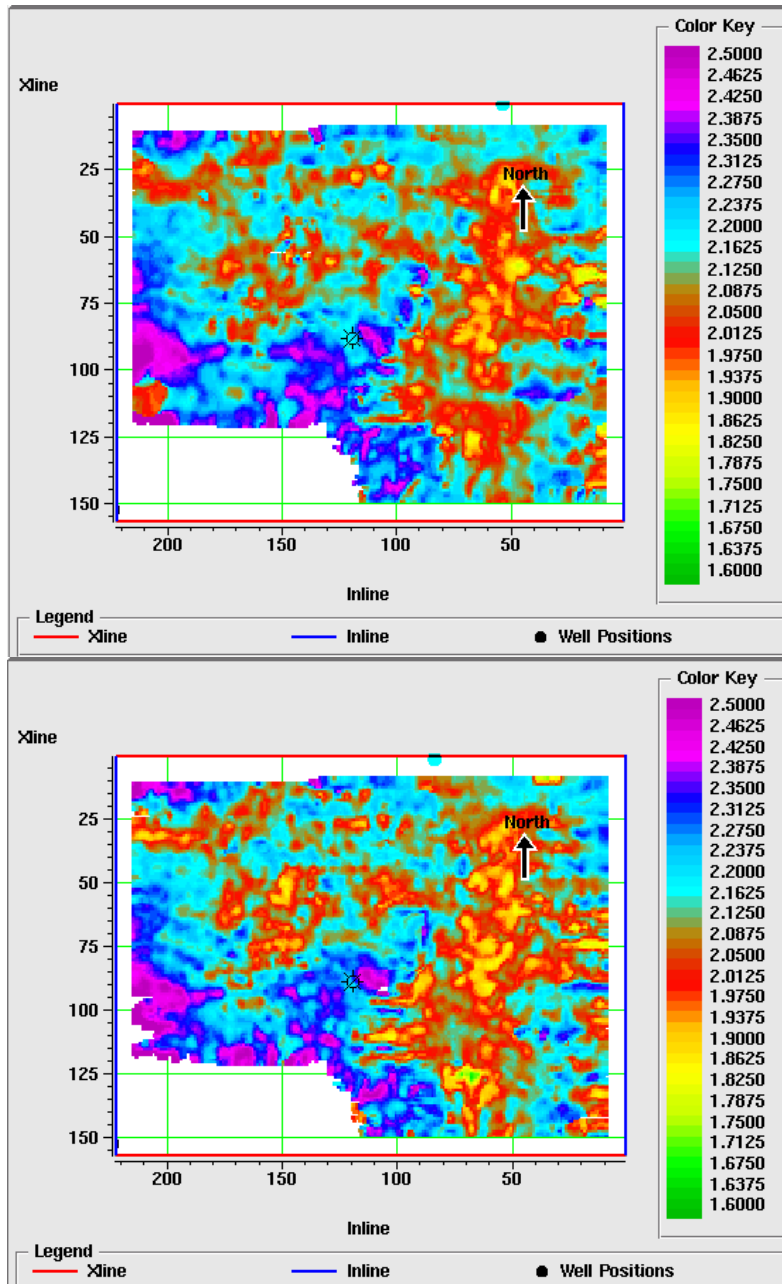


FIG 19. Interval V_p/V_s map from the Birdbear Formation to the Dawson Bay Formation. a: 2004 survey; b: 2008 survey.

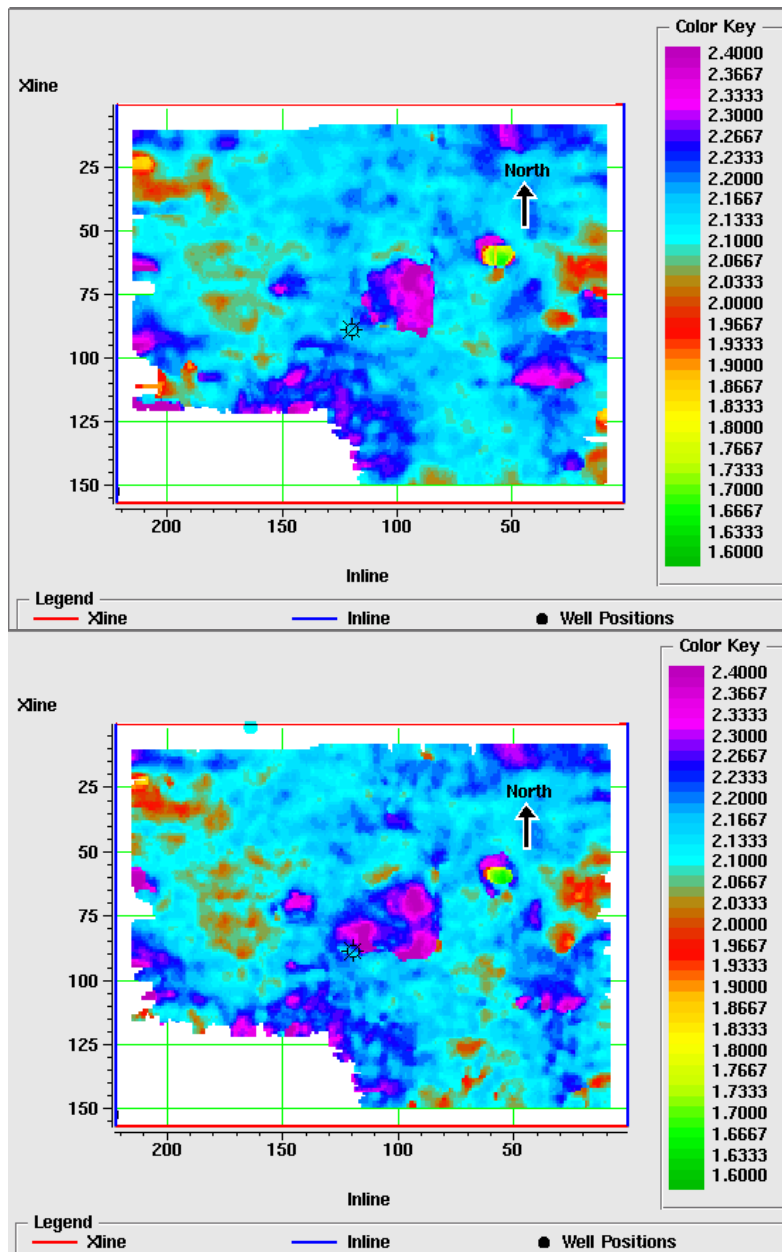


FIG 20. Interval Vp/Vs map from the Birdbear Formation to the Shell Lake anhydrite. a: 2004 survey; b: 2008 survey.

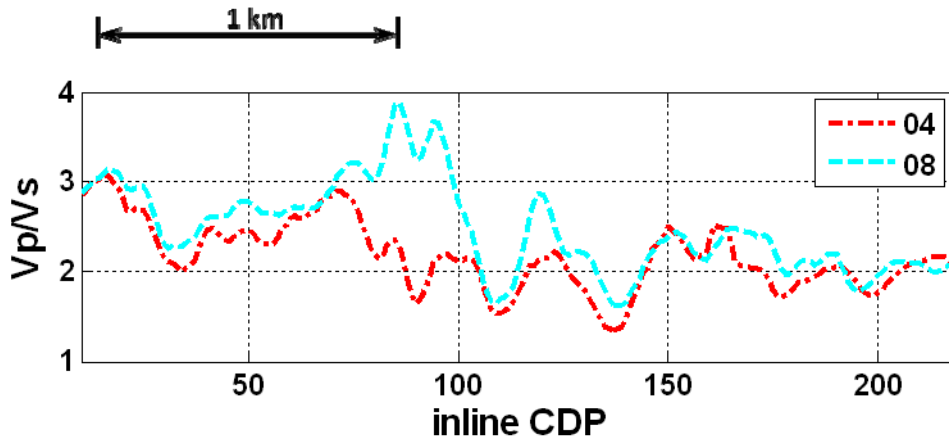


FIG 21. Average Vp/Vs values of west-east line 89 between the bottom of the Porous zone and the top of Prairie Evaporite Formation. The red line denotes the values from the 2004 survey, the blue line shows the values of the 2008 survey.

Fracture detection using curvature

Compared with coherency methods, reflector curvature is a seismic attribute relating more directly to fracture distribution (Lisle, 1994; Roberts, 2001). It helps to remove the regional dip effects and emphasizes the small scale features (Ganguly et al., 2009). It can be used to quantify the distribution of brittle strain in strata and thus can be used to predict fracture orientations and distributions. The most positive and negative curvatures were found to be the most useful for delineating faults, fractures, flexures, and folds (Al-Dossary and Marfurt, 2006). To delineate the fractured zone which could pose a brine inflow problem to potash mining, the curvature attribute is calculated for the top of the Dawson Bay Formation and the mining level on 2008 radial data (FIG 22 and FIG 23). Compared with the top of the Dawson Bay Formation, the curvature calculated at the mining level shows a more intense possible zone of fractures. This indicates that above the Dawson Bay Formation, fractures are rare, but are interpreted to be well developed in the Dawson Bay Formation and at the mining level. Curvature values also showed the distribution patterns of the fractured zone: around the edge of the trap door area, fractures were well developed; another fractured zone lies at the top right corner of the survey, which can also be easily seen on the time difference map of the mine level between 2004 and 2008 radial component data (FIG 17c).

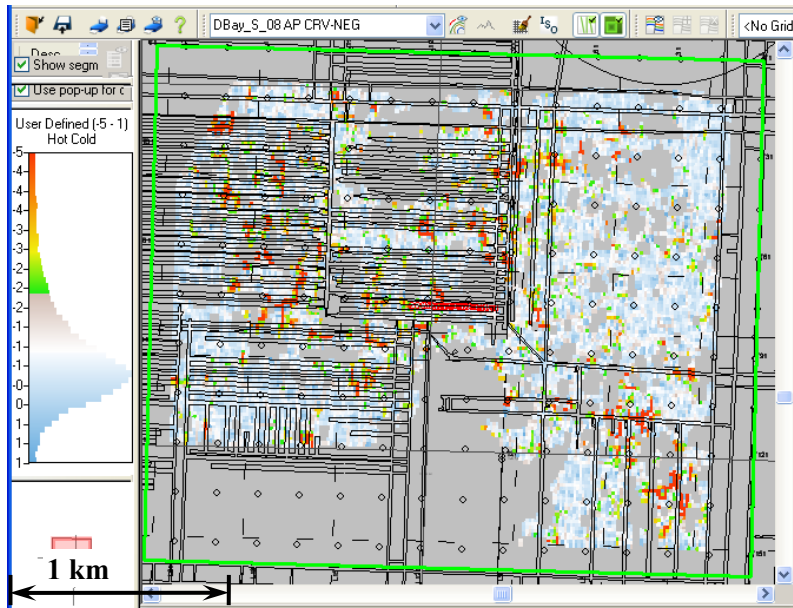


FIG 22. Negative curvature of the Dawson Bay Formation on PS data of the 2008 survey.

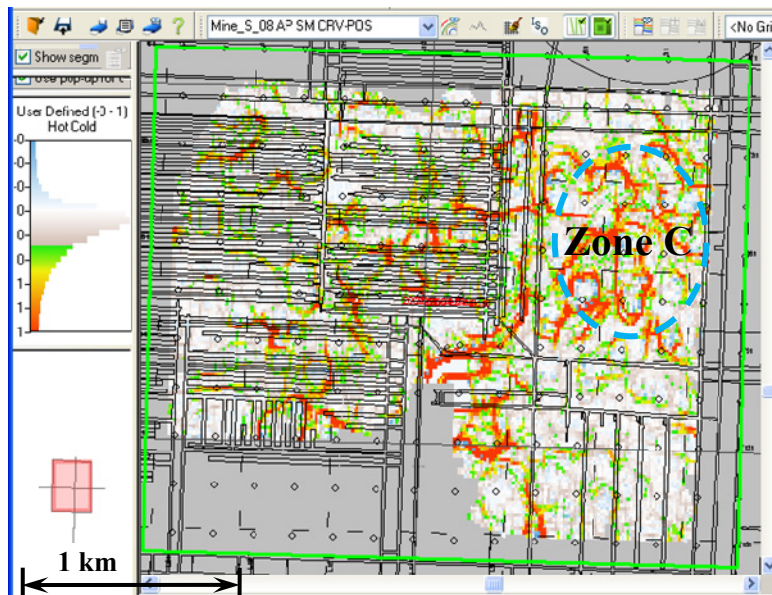


FIG 23 Positive curvature of the mine level on PS data of the 2008 survey.

Discussion

The seismic signatures of the fractures were interpreted from various analyses of the time-lapse 3C-3D seismic survey. The match filters were derived in a window from 420-620 ms for vertical data, and 600-1250 ms for radial data respectively. From the time shift and amplitude difference, there were also some changes of the strata between the Birdbear Formation and the Dawson Bay Formation. To separate the difference caused by the fractures in the Dawson Bay Formation, the windows for match filter calculations are relatively narrow. It is best to calculate the filter from the top of the Devonian to the top of the Dawson Bay Formation.

Curvature has proved to be an effective attribute to delineate the fractures in this study. Since they were only calculated using the full wave-bandwidth data, we are confident on detecting the overall fracture effect. To account for subtle features at different wavelengths, it might be better to examine curvature at various scales.

CONCLUSION

The PP and PS synthetic seismograms correlate reasonably well with field time-lapse 3C-3D surface seismic data. Noticeable amplitude changes and push-down effects can be seen on the time-lapse 3C-3D surveys at the Dawson Bay and underlying formation in the 2008 survey compared with the 2004 survey, especially on the PS data. Increasing Vp/Vs values can be found on the 2008 survey within the trap door area. Seismic curvature attributes calculated at the top of the Dawson Bay Formation and the mining level also suggest that the fractures are well developed in the Dawson Bay Formation.

ACKNOWLEDGEMENTS

We thank Mr. John Boyd for assisting with access to seismic data from Mosaic and also for valuable discussions. The support by the sponsors of the CREWES project is gratefully appreciated. Software used for this paper was kindly provided by Zokero (Seisware), and Hampson Russell Software Services.

REFERENCES

- Al-dossary, S., and Marfurt, K. J., 2006, 3D multispectral estimates of reflector curvature and rotation: *Geophysics*, 71, 41-51.
- Fuzesy, L.M., 1982, Petrology of potash ore in the Esterhazy Member of the Middle Devonian Prairie Evaporite in southeastern Saskatchewan: *Proceedings of the Fourth International Williston Basin Symposium*, 67-73.
- Ganguly, N., Dearborn, D., Moore, M., Gordon, D., Horan, M., and Chopra, S., 2009, Application of seismic curvature attribute in the appraisal of the Tishrine-West field, North-East Syria: *Recorder*, 34, 29-43.
- Margrave, G.F., Lawton, D.C., and Stewart, R.R., 1998, Interpreting channel sands with 3C-3D seismic data: *The Leading Edge*, 17, 509-513.
- Zhang, Z., and Stewart, R.R., 2009, Seismic detection of cracks in carbonates associated with potash mining: 2009 CSEG Annual Convention, Expanded Abstracts.
- Zhang, Z., Lawton, D.C., and Stewart, R.R., 2010, Numerical modeling of shear-wave splitting and azimuthal velocity analysis in fractured media: 2010 CSEG Annual Convention, Expanded Abstracts.